A combined model for improving estimation of atmospheric boundary layer height

by Vera Surtia Bachtiar

Atmospheric Environment 98 (2014) 461–473

Contents lists available at ScienceDirect

Atmospheric Environment

journal homepage: www.elsevier.com/locate/atmosenv

A combined model for improving estimation of atmospheric boundary layer height

V.S. Bachtiar [a, *], F. Davies [b], F.M. Danson [b]

[a] Air Quality Laboratory, Environmental Engineering, Andalas University, Padang, Indonesia
[b] School of Environment and Life Sciences, University of Salford, Salford M5 4WT, UK

HIGHLIGHTS

- Comparison boundary layer height from ADMS 4 and lidar measurement.
- Develop a combined model to improve atmospheric boundary layer height prediction.
- Comparison boundary layer height from the combined model and lidar measurement.
- The combined model improve the prediction of the atmospheric boundary layer height.

ARTICLE INFO

Article history:
Received 13 May 2014
Received in revised form
6 September 2014
Accepted 9 September 2014
Available online 10 September 2014

Keywords:
Boundary layer height
ADMS
Lidar
Combined model

ABSTRACT

Atmospheric boundary layer height is one of the most important parameters in atmospheric dispersion modelling because it has a large effect on predicted air quality. Comparisons between Atmospheric Dispersion Modelling System, version 4 (ADMS 4) and lidar data were carried out on boundary layer height data from central London. The comparison showed that the boundary layer height predicted by the ADMS 4 was, on average, lower than lidar for the subset of data taken. ADMS 4 has a very simple surface scheme which is not representative of complex urban environments and the results from this research imply that there is not sufficient surface roughness within the model to produce a large enough boundary layer height. The aim of this study is to create an improved model to better forecast the growth of the daytime urban boundary layer and predict boundary layer height, h, in an air quality dispersion model using lidar measurements. The combined model was developed by using a surface model and an atmospheric boundary layer height model. Measurements of atmospheric boundary layer height by lidar used vertical velocity variance and the overall conclusion was that the combined model improved the performance of ADMS in urban areas.

1. Introduction

Development within urban areas is inevitably followed by the problem of air pollution. Air pollution problems attract more attention from around the world because they have a detrimental effect on humans and the environment. In the 20th century, air pollution problems have occurred around the world and the World Health Organisation (WHO) confirm that air pollution is a major environmental risk to health causing approximately two million premature deaths worldwide per year (WHO, 2008). In an effort to assess the effects on human health caused by air pollution, United Kingdom (UK) authorities use a combination of monitoring and modelling of air quality. Monitoring is carried out for current air quality and modelling is used to gauge current air quality in locations where no monitoring equipment is available, or for future air quality purposes. Modelling air quality to predict air pollution incidents has been used since the late 1950s, when atmospheric dispersion models were used to predict air quality. The first model was developed by Pasquill in the UK, and extended by Gifford in the USA and others elsewhere (Carruthers et al., 1994). A number of models for predicting air quality have been developed around the world. In the USA, improving national air quality is done by modelling new and existing air pollution sources for compliance with the National Ambient Air Quality Standards (NAAQS) (U.S. EPA, 2008). The UK has used a combination of monitoring and modelling for air quality management, under Part IV of the Environmental Act 1995. In the air quality strategy for England, Scotland, Wales and

* Corresponding author.
E-mail addresses: vera.surtia@gmail.com, vera_sb@ft.unand.ac.id (V.S. Bachtiar).

http://dx.doi.org/10.1016/j.atmosenv.2014.09.028
1352-2310/

Northern Ireland, there is also a process for national modelling for future air quality (DEFRA, 2007).

The use of atmospheric dispersion models for predicting air quality is essential for developing the UK air quality strategy and local authorities have routinely used dispersion models and in particular the Atmospheric Dispersion Modelling System (ADMS) (Davies et al., 2007). ADMS is a computer code for modelling the dispersion of gases and particles emitted into the atmosphere (Carruthers et al., 1994). ADMS has a number of component modules, one of which is a meteorological pre-processor that allows a variety of meteorological data to be input or calculated, including atmospheric boundary layer height (h) which is a key parameter required for correct predictions of air pollution concentrations. h is an important parameter in dispersion models because it determines the height of spread of aerosols and pollutants, and effectively determines the volume available for pollutant dispersion, although this also depends on meteorological parameters, surface turbulent fluxes and physical parameters (Fisher et al., 2005). The limits on the vertical diffusion of the plume of material released are determined by h. In ADMS, h is also used to calculate other meteorological parameters, such as turbulence, wind speed, velocity, heat, moisture and momentum (Dandao et al., 2009).

The accuracy of predicted h is important in urban air quality modelling because it affects near-surface pollutant concentration predictions (Dandao et al., 2009). As an example, a large difference in pollutant concentrations was found between ADMS 3.1 and AERMOD PRIME 02222 when modelling emissions from tall stacks (Sidle et al., 2004). It was found that the difference in predicted concentrations was due to the different predictions of h within the models. h can be determined by atmospheric dispersion models but the estimation of h by these models may be incorrect. Davies et al. (2007) compared estimated h from the UK Meteorological Office Unifed Model (UM) and ADMS, to pulsed Doppler lidar measurements. ADMS was run under three settings, an 'urban' roughness, a 'rural' roughness and a 'transition' roughness ('transition' means meteorological data from an airport but pollution dispersion from over a city). The results showed that occasionally h was overestimated by the UM model. Meanwhile, ADMS gave accurate results in predicting h for the rural and transition settings, but overestimated h for the urban setting. Based on the evidence that dispersion models still cannot accurately predict boundary layer height in urban areas, it is necessary to analyse this parameter further. The aim of this study was to create an improved model to better forecast the growth of the daytime urban boundary layer in an air quality dispersion model, and to use lidar measurements to validate the new model.

2. Methods

This study is split into three stages: Stage 1 is a comparison of the boundary layer height from ADMS 4 and from lidar vertical velocity variance measurements; Stage 2 shows the development a combined model for improving atmospheric boundary layer height prediction – the new model is a combination of the surface model from Grimmond and Oke (1999), and the atmospheric boundary layer height model from Batchvarova and Gryning (1991); Stage 3 is a comparison of the boundary height from the combined model and lidar vertical velocity variance measurements. This study focuses on the growth of the atmospheric boundary layer height from sunrise in fully convective conditions. Therefore, the data used was between 08:00 and 14:00 local time. This because, it is assumed under the particular conditions of the measurements, the atmospheric boundary layer height starts to grow at 08:00 and reaches a peak height at 14:00 local time. It is important for dispersion models to estimate the correct h in this time range because, under convective conditions, morning boundary layer growth is crucial in determining the development and final maximum height.

2.1. Study area and data

For this study lidar data were derived from the Salford University Halo lidar manufactured by Halo Photonics Ltd. and operated as part of the UK University Facility for Atmospheric Measurement (UFAM) instrument pool (Pearson et al., 2009). The instrument has been deployed in various activities, including atmospheric boundary layer monitoring at the Salford University Urban and Built Environment Research Base (SUBERB) in 2006 (Bozier et al., 2006), observation of Russian forest fire plumes over Helsinki in 2007 (Bozier et al., 2007), and the Convective and Orographically Induced Precipitation Study (COPS) in Germany in 2007 (Wulfmeyer et al., 2008).

The data used in this research were collected for the Regent's Park and Tower Environmental Experiment (REPARTEE) II campaign, which was an experiment to study atmospheric chemical processes and parameters which affect atmospheric aerosol concentrations in London (Barlow et al., 2011). The meteorological instruments employed in the REPARTEE II campaign and used in this study were a three-axis ultrasonic anemometer (R3-50) and weather station (Vaisala WXT510), installed on the top of the British Telecom Tower (latitude 51° 31′ 17.31″N and longitude 0° 8′ 20.12″W, 1.2 km to the east of the lidar site) (Barlow et al., 2011). The lidar data were collected using the Salford Halo Lidar which was installed in a car park at the University of Westminster on Marylebone Road (latitude: 51° 31′ 20″N and longitude: 0° 09′ 22″ W). The instruments were run continuously for three weeks between 24th October and 14th November 2007.

For the London case study, local surface meteorological data were not available. It is not standard procedure for the UK Met Office to collect meteorological data in urban centres as data taken from such sites is influenced by local effects such as shadowing and hard surfaces. Consequently no meteorological data was taken at the lidar site at the University of Westminster. The lack of meteorological data was overcome by using surface meteorological data from stations around London. These meteorological data are standard Met Office measurements, taken from the surface meteorological site at Northolt (latitude: 51° 32′ 55″ N and longitudinal: 0° 25′ 1″ W).

The Northolt meteorological location is in an airport area. The surface roughness length, z_0, at the airport is very low and has a value of 0.02 m (the value chosen in ADMS 4 for fairly smooth grassland). Meanwhile, the surface roughness in the pollution site (lidar location) was set to an urban area surface roughness, $z_0 = 1.5$ m (the value chosen in ADMS 4 for urban areas). ADMS 4 uses input meteorological data, such as wind speed (m/s), wind direction (degrees), cloud amount (oktas), temperature (C), sensible heat flux (W/m^2), precipitation rate (mm/hour) and relative humidity (%). ADMS allows inputs for both the meteorological site and the pollution site and allows each site to have different roughness lengths. This allows for the situation where pollution dispersion is occurring over, for example, an industrial power plant, but the meteorological data is being collected from the nearest airport site.

2.2. The combined model

Most computational algorithms within dispersion models for predicting surface layer behaviour are based on empirical models of relatively smooth surfaces. Therefore there has been much work recently on urban surface morphology and dispersion of pollution

in urban areas. The aim of this work was to first assess the performance of a routinely used dispersion model with 'urban settings' against lidar measurements of boundary layer height. Second two separate models were coupled together to produce an urban surface model of boundary layer height growth. Third the new model was be tested and validated with lidar data and surface morphology statistics from central London. The structure of the combined model for estimation of the atmospheric boundary layer height is presented in Fig. 1.

Step 1 of the model is a surface roughness calculation. Surface roughness is a very important parameter influencing the surface wind shear in the surface layer. In typical dispersion models, like ADMS 4, the settings for surface roughness are very simple. The surface roughness element of the model is designed so that a more realistic representation of the urban surface layer can be modelled. The details of this are contained in section 2.3. The resulting value of surface roughness length is then used as the input for calculation of friction velocity in the next step.

The second step is a calculation of the friction velocity. Friction velocity, sometimes referred to as shear velocity, is a measure of magnitude of the horizontal Reynolds stress vector in the direction of the mean wind (Stull, 1988). The friction velocity is calculated here using two methods: an iterative method and use of the mean wind speed. Details of these are contained in section 2.4. The outputs of friction velocity are used as input for calculation of the atmospheric boundary layer height.

Monin–Obukhov length describes the effects of turbulent flow in the surface layer and is the height at which turbulence is generated more by buoyancy than by wind shear. Calculation of Monin–Obukhov length is carried out in the second step. Initially, both the friction velocity and Monin–Obukhov length values are calculated for neutral conditions. Then calculations for friction velocity and Monin–Obukhov length are carried out iteratively until the results converge and the difference is not more than 1%. In each iteration, the last value of the Monin–Obukhov length in an iteration, become the new value for the next iteration. Monin–Obukhov length value is then used as an input for calculation of the atmospheric boundary layer height.

In module 3 of the combined model a calculation of the potential temperature gradient above the atmospheric boundary layer (γ) is carried out. Gamma represents the potential temperature gradient in the stable boundary layer and is a measure of the energy needed for the entrainment process while the mixed layer is growing. Therefore, gamma should represent the temperature gradient in the stable layer (Gryning, 2005). To determine gamma in the stable layer, measurement of the temperature profile for gamma using radiosonde is generally taken in the morning and is assumed to be constant during the days (He et al., 2006). In this study, the sounding data used were measured around six o'clock in the morning. In this calculation, temperature and pressure from radiosonde measurements are required as input data. The temperature data was derived from radiosonde data from Larkhill,

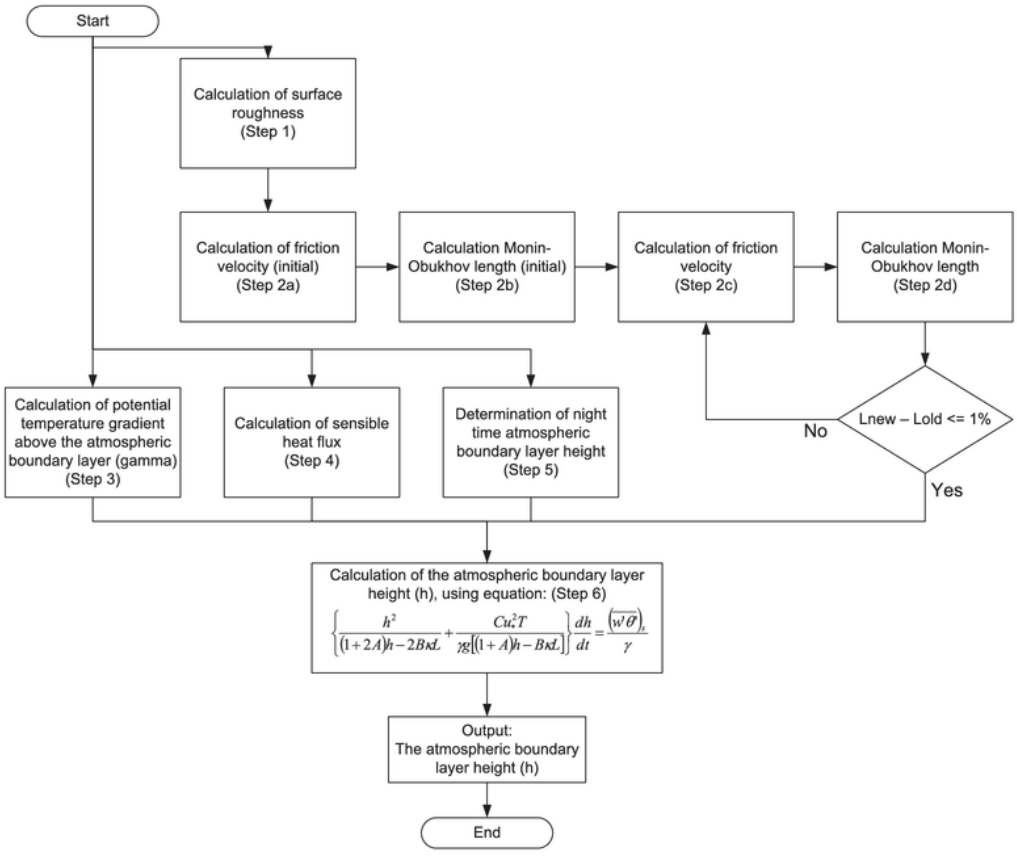

Fig. 1. The structure of model for calculation of the atmospheric boundary layer height.

taken from the BADC (2010). The output γ is used as input for the calculation of atmospheric boundary layer height.

Step 4 of the combined model is calculation of sensible heat flux for central London. Sensible heat flux is a heat from anthropogenic sources and solar input (Kato and Yamaguchi, 2005). Sensible heat flux was calculated using data from Northolt (assumed to represent a suburban area) and modified to determine a sensible heat flux for central London (urban area). The fifth step of the structure model is a calculation of the night time boundary layer height. The night time boundary layer height was required to determine the height of atmospheric boundary layer in the stable condition, where turbulent fluxes are nearly constant (Arya, 2005).

The output of the combined model is atmospheric boundary layer height. This model can be used to predict the growth of atmospheric boundary layer height in unstable conditions. The model was therefore developed based on combining a surface model and an atmospheric boundary layer height model.

2.3. Calculation of surface roughness

Urban areas have the largest surface roughness length compared with other surface types (Wieringa, 1993). This is caused by the size of the roughness elements (buildings etc) of the cities and has major implications for surface drag, momentum transport, scales and intensity of turbulence, and mass convergence (uplift) and divergence (subsidence). Hence, it is vital to have an accurate knowledge of aerodynamic characteristics of cities for describing, modelling and forecasting the behaviour of urban winds and turbulence at all scales. Unfortunately, the ability to assign values of surface roughness length remains problematic.

There are two classes of method available to assign values of surface roughness length. First, micrometeorological (or anemometric) methods that use field observations of wind or turbulence to estimate aerodynamic parameters included in theoretical relations derived from the logarithmic wind profile. Second, morphometric or geometric methods that use algorithms that relate aerodynamic parameters to measures of surface morphology. Micrometeorological methods have the advantage that the characteristics of the surface do not need to be specified (the roughness elements can consist of any combinations and can be arranged in any pattern). The disadvantages are that measurements of surface roughness are dependent on wind direction and speed and also upwind fetch. This makes the measurements only valid for a small area and so many measurements must be made. City centres have many varied neighbourhoods and surface roughness differs enormously. In cities the expense and difficulty involved in obtaining and operating a field site is very high (particularly when installing a tower in a city). Furthermore, results must be obtained for all wind directions (Grimmond and Oke, 1999).

Morphometric methods have the advantage that the values can be determined without the need of tall towers and instrumentation. Furthermore, if a spatially continuous database of the distribution of roughness elements is available, then values can be computed for any directions surrounding the site of interest. One of the disadvantages of this method is it requires simplified simulations of wind direction and roughness elements. In these simulations, the flow is assumed to be constant in direction, typically normal to the face of the elements, and the buildings are assumed to be arrayed in regularly spaced rows or grids. These conditions are different from real cities where wind direction is not constant, and shape of individual roughness elements are not regular (Grimmond and Oke, 1999).

According to Grimmond and Oke (1999), it is difficult to decide which method is more accurate. Nevertheless in this study, the calculation of surface roughness in urban areas used morphometric methods, based on its simplicity and cost effectiveness and the fact that the calculations surface roughness are better suited to urban surfaces because they take into account both building height and density. This method yields values of surface roughness for all directions around a site and can be derived for a particular city region. In this method, the surface roughness is calculated using the height of the surface roughness elements, $\overline{z_H}$, and frontal area index, $\overline{\lambda_F} = \overline{A_F}/\overline{A_T}$, where $\overline{A_F}$ is the mean area of the surface elements facing the wind and $\overline{A_T}$ is the mean footprint area of the elements array (Fig. 2).

The frontal area index, which combines mean height, breadth and density of roughness elements, is defined as:

$$\overline{\lambda_F} = \overline{L_y}\,\overline{z_H}\rho_{el} = \overline{L_y}\,\overline{z_H}\Big/\overline{D_x D_y} \tag{1}$$

Where $\overline{L_y}$ is the mean breadth of the roughness elements perpendicular to the wind direction, ρ_{el} is the density (number (n) of roughness elements per unit area ($\rho_{el} = n/A_T$)), $\overline{D_x}$ is the average inter-element spacing (between element centroids) in the along wind direction, and $\overline{D_y}$ is the average in the crosswind direction (see Fig. 2). The typical values of frontal area index are in the range 0.1–0.25 for crops, about 1–10 for forests (Raupach, 1991), and between 0.1 and 0.3 for urban areas, with individual sectors varying from 0.06 to 0.4 (Grimmond and Oke, 1999).

The surface roughness was calculated using the Raupach method (1992) (Grimmond and Oke (1999). According to Grimmond and Oke (1999), this method is one of the best three methods currently available. Input requirements for this method are relatively simple and this method applies across the full range of roughness densities. The method is described in the following equations:

$$\frac{z_d}{z_H} = 1 + \left\{\frac{\exp\left[-(c_{d1}2\lambda_F)^{0.5}\right] - 1}{(c_{d1}2\lambda_F)^{0.5}}\right\} \tag{2}$$

$$\frac{z_0}{z_H} = \left(1 - \frac{z_d}{z_H}\right)\exp\left(-k\frac{U}{u_*} + \psi_h\right) \tag{3}$$

The element portrayed has the characteristic mean dimensions, spacing and total area (AT) of the urban array. Using these measurements, the following non-dimensional ratios are defined to characterize the morphometry: $\overline{\lambda_P} = \overline{A_P/A_T} = \overline{L_x L_y/D_x D_y}$, $\overline{\lambda_F} = \overline{A_F/A_T} = \overline{z_H L_y/D_x D_y}$, $\overline{\lambda_S} = \overline{z_H/W_x} = \overline{z_H/D_x - L_x}$, and $\overline{\lambda_C} = [\overline{L_x L_y} + 2(\overline{L_y z_H}) + 2(\overline{L_x z_H})/\overline{D_x D_y}]$ (Grimmond and Oke, 1999).

Where z_d is zero-plane displacement length, z_H is building height, z_0 is roughness length, $u_*/U = \min\left[(c_s + c_R\lambda_F)^{0.5}, \left(\frac{u_*}{U}\right)\max\right]$, $\overline{\lambda_F} = \overline{A_F}/\overline{A_T} = \overline{z_H L_y}/\overline{D_x D_y}$ (see Fig. 2), λ_F is the frontal area index, ψ_h the roughness sub layer influence function ($\psi_h = 0.193$), U is the large-scale wind speed, u_* is the friction velocity, c_s and c_R are drag coefficients for the substrate surface at height z_H in the absence of roughness elements and of an isolated roughness element mounted on the surface ($c_s = 0.003$ and $c_R = 0.3$), c_{dl} is a free parameter ($c_{dl} = 7.5$), and $(u_*/U)_{\max} = 0.3$ (Grimmond and Oke, 1999). In this study, λ_F was calculated using building statistics of the area where the lidar was located (Marylebone Street, London). Surface roughness was calculated for an area of 1 km^2 around the lidar location. The building height data was derived from MIMAS (2010), was analysed using ArcMap (See Fig. 3).

The number of buildings selected by ArcMap for the 1 km^2 was 900. The heights of the buildings ranged between 3.7 m and 67.1 m and had a mean height of 20.131 m. The distribution of heights is shown in Fig. 4. The percentages of heights of the buildings in this area were as follows; 6% of the buildings were below 10 m, 16% were between 10.1 and 15 m, 34% were 15.1–20 m, 26% were

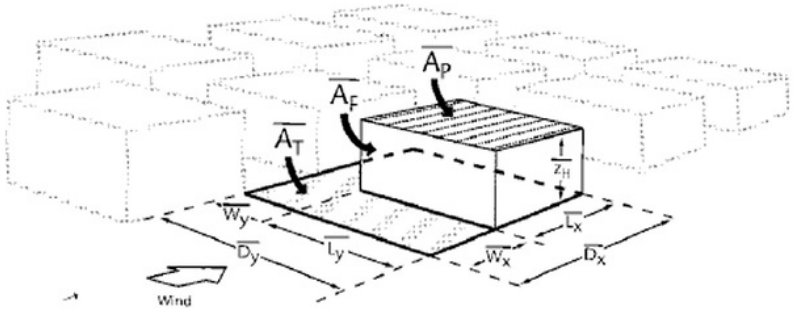

Fig. 2. Definition of surface dimensions used in morphometric analysis.
(Source: Grimmond and Oke, 1999).

20.1–25 m, 11% were 25.1–30 m, 5% were 30.1–35 m, and 3% were 35.1 m or above.

In real cities the positions of buildings are of course not always arranged facing the mean wind as ideally required for the morphometric methods. Therefore in this study, the positions of buildings were simplified. For calculation of λ_F, the lengths of the buildings were assumed to be twice their width. It was assumed that half the buildings had their lengths perpendicular to wind direction and the other half had their widths of building perpendicular to wind direction (Fig. 5). The surface roughness length from this calculation was 2.4 m. This value was much higher than the surface roughness length setting in ADMS 4 for 'large urban area' of 1.5 m.

2.4. Calculation of friction velocity and Monin–Obukhov length

Calculation of friction velocity can be carried out using two methods: first using the mean of wind speed, $\overline{M}$, as a function of height, z (Stull, 1988) and second by iteration (Fatogoma and Jacko, 2002).

2.4.1. Calculation of friction velocity using mean wind speed

Stull (1988) formulated $\overline{M}$ from surface roughness (z_0), height (z), friction velocity (u^*) and wind speed (u) as follows:

$$\frac{\overline{M}}{u^*} = \left(\frac{1}{k}\right)\ln\left(\frac{z}{z_0}\right) \tag{4}$$

where k is the von Karman constant (=0.4). From equation (4):

$$u^* = \frac{\overline{M}}{\ln\left(\frac{z}{z_0}\right)}k \tag{5}$$

So, friction velocity (u^*) can be determined from the gradient of the line as shown in Fig. 6.

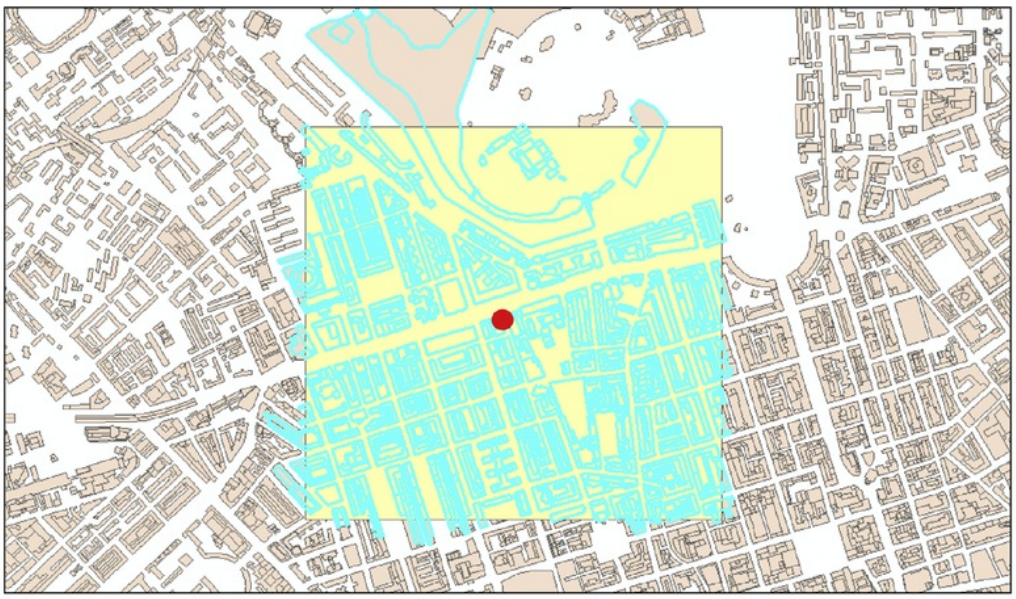

Fig. 3. Buildings selected by Arcmap for 1 km^2 (red dot is the lidar location). (For interpretation of the references to colour in this figure legend, the reader is referred to the web version of this article.)
Source: MIMAS (2010)

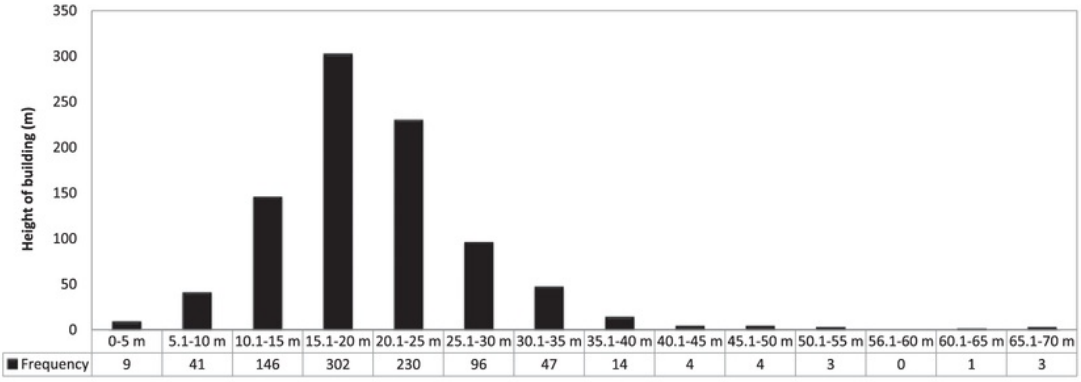

Fig. 4. The number of buildings against height.

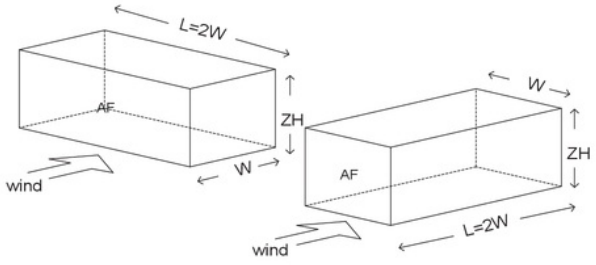

Fig. 5. Illustration of position of buildings against wind direction (AF = area of buildings perpendicular to the wind direction).

Fig. 6 shows the estimation of $\overline{M}$ by plotting wind speeds against ln (z/z_0) for 29th October 2007 at 14.00 data. The values of friction velocity were acquired from $\overline{M}$ values. The wind speeds were derived from the Salford Halo Doppler Lidar measurements, in Marylebone, central London. Fig. 7 shows the profile of wind speeds on 29th October 2007 at 14.00.

2.4.2. Calculation of friction velocity using iteration

By iteration, friction velocity is calculated in parallel with Monin-Obukhov length. The input data needed for this calculation are wind speed, temperature, sensible heat flux, and surface roughness length. These data were obtained from the surface measurements from the Northolt Meteorological Station. Meanwhile, the surface roughness length was calculated in section 2.3. The friction velocity for this calculation is a function of the vertical profile of wind speed:

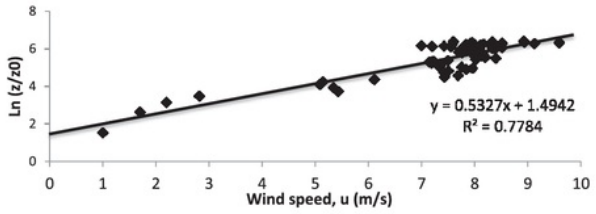

Fig. 6. Wind speeds against log (z/z_0) on 29/10/2007 at 14:00. (red line is $\overline{M}$ that is made using linear regression of wind speeds against ln (z/z_0)).

$$u* = kU_z\left[\ln\left(\frac{z}{z_0}\right) - \psi_M\left(\frac{z}{L}\right) + \psi_M\left(\frac{z_0}{L}\right)\right]^{-1} \tag{6}$$

where U_z is the wind speed at given height z, $k \approx 0.4$ is the von Karman constant, z_0 is the surface roughness length, and ψ_M is a momentum stability parameter. When $1/L < 0$ (unstable condition):

$$\psi_M = 2\ln\left(\frac{1+x}{2}\right) + \ln\left(\frac{1+x^2}{2}\right) - 2\tan^{-1}(x) + \frac{\pi}{2} \tag{7}$$

where: $x = \left(1 - 16\frac{z}{L}\right)^{1/4}$

When $1/L > 0$ (stable condition):

$$\psi_M = -5\frac{z}{L} \tag{8}$$

The Monin–Obukhov length is defined as:

$$L = -\frac{\rho c_p T u_*^3}{kgH} \tag{9}$$

Calculation of the Monin–Obukhov length (L) was performed using the iteration method (Fatogoma and Jacko, 2002). The

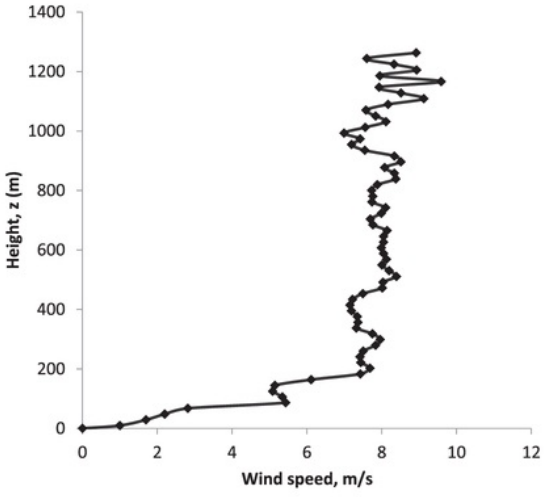

Fig. 7. Wind speed measurement by lidar on 29/10/07 at 14.00.

iteration was started assuming neutral conditions by estimating $u\times$with $\psi_M = 0$ in equation (6). Reference height (z) was started at 67.493 m which is the minimum height of wind speed measurement from lidar above the building height. Then, L was calculated from equation (9). The new value of L was substituted in equations (6)–(9) to obtain improved values of u^*. This cycle was repeated until there was only 1% difference between the two values of L.

Calculations of friction velocity using both methods were compared. Overall, the friction velocity derived by mean wind speed was higher than the friction velocity by iteration. The friction velocity by mean wind speed and iteration, produced similar values of atmospheric boundary layer height (h) in the combined model. However, the h values derived from the friction velocity obtained from iteration was chosen to compare with h lidar vertical velocity variance because the required Monin–Obukhov length values were also obtained from the iterations procedure.

For Monin–Obukhov length, there was no alternative measurement data available. So, as well as friction velocity, the values of Monin–Obukhov length for running the combined model were calculated using iteration. The values of Monin–Obukhov length (L_{MO}) at 08:00 at each date were stable, since the values of L_{MO} were positive. On the other hand, L_{MO} of the calculation at each date after 08:00 were unstable. The values calculated were negative and the values of L_{MO} are very high at 09:00 and 10:00 due to very low sensible heat fluxes (close to zero). L_{MO} was also negative at 11:00 to 14:00 meaning unstable conditions at these times.

2.5. Calculation of sensible heat flux

Sensible heat flux was calculated based on the difference of the values of sensible heat flux between urban and rural areas. According to Fisher et al. (2005), the sensible heat flux in urban areas is higher than the sensible heat flux in rural areas. The increase of sensible heat flux in urban areas in the morning and the decrease in the evening are later than in rural areas. In urban areas, the later rise of sensible heat flux compared to rural areas is caused by shadowing effects. These affect the temperature in urban areas, and therefore delay the increase of sensible heat flux (Dupont et al. 2004). In the case of sensible heat flux obtained from rural or suburban sites, the values need to be modified in order to be used as proxies for urban values.

In this study, sensible heat flux was derived from Northolt data because there are no meteorological measurements in central London. The Northolt data was assumed to be data from a suburban area and was modified as follows:

(i) Calculate the percentage difference each hour of sensible heat flux (H) between Northolt and Andrewsfield for the 6 days of interest(Andrewsfield was taken as a rural site typical of the area)
(ii) Average the percentage difference over the 6 days for each hour (8am–2pm)

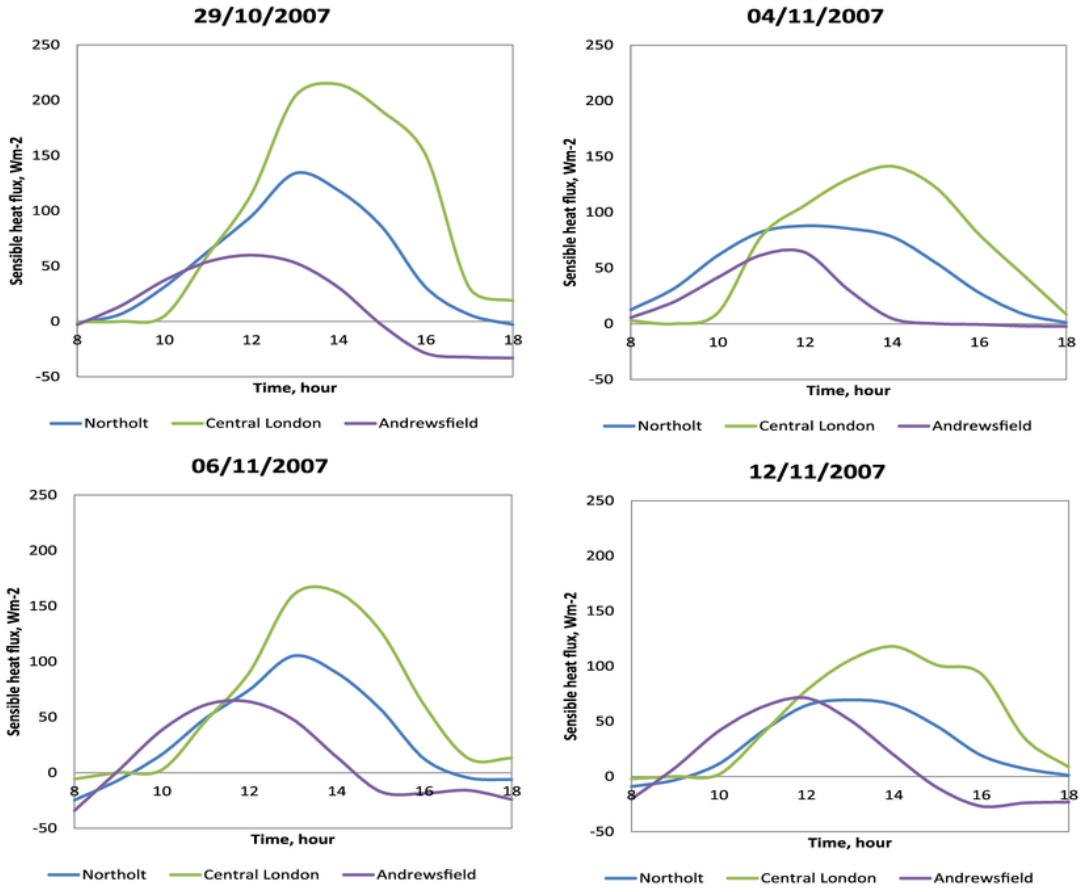

Fig. 8. Sensible heat flux measured for Andrewsfield (rural) and Northolt (suburban), and calculated for Central London (urban).

(iii) Calculate increasing sensible heat flux every hour by multiplying Northolt sensible heat flux and average of the percentage different in step 2.
(iv) Sensible heat flux of urban areas is obtained by adding sensible heat flux from Northolt and the increase of sensible heat flux in step 3.

The result of modified sensible heat flux can be seen in Fig. 8. It can be seen that there is a time lag and increasing sensible heat flux in urban areas compared with the data from Northolt.

2.6. Calculation of potential temperature gradient above the atmospheric boundary layer

In this study, the atmospheric boundary layer height model from Batchvarova and Gryning (1991) was adopted. In this model, potential temperature above the atmospheric boundary layer is an important parameter to calculate the atmospheric boundary layer height. As the boundary layer top increases in height due to increased instability and turbulence within the boundary layer it entrains the stable layer directly above it. The stability in the region directly above the developing boundary layer top is therefore an important parameter in affecting the speed of development of the boundary layer.

In this study, the potential temperature gradient above the atmospheric boundary layer (termed Gamma) was determined from radiosonde data from the Larkhill (122 km from Marylebone Road, London) which was the closest radiosonde site to the lidar site. The radiosonde data were taken from the BADC (2010). Gamma represents the potential temperature gradient in the stable boundary layer and is a measure of the energy needed for the entrainment process while the mixed layer is growing. To determine Gamma in the stable layer, measurement of the temperature profile for Gamma using radiosonde is generally taken in the morning and is assumed to be constant during the days (He et al., 2006). In this study, the sounding data used were measured starting at six o'clock in the morning (local time).

The potential temperature was calculated using equation (AMS, 2009):

$$\theta = T\left(\frac{p_o}{p}\right)^{\kappa} \tag{10}$$

where θ is the potential temperature (K), T is temperature (K), p_o is standard pressure (=100 kPa), p is pressure (Pa), and κ is Poisson constant (the ratio of the gas constant to the specific heat at constant pressure) which is assumed to be 2/7 (AMS, 2009). The potential temperature against height at Larkhill can be seen for three separate days in Fig. 9.

The potential temperature gradient above the atmospheric boundary layer height (Gamma) was calculated from the potential temperature per height (°K/m). The Gamma used for modelling can be seen in Table 1. It can be seen that the values of Gamma range between 0.0028 and 0.0038.

2.7. Determination of night time atmospheric boundary layer height from lidar

At night, the stable boundary layer is characterized by a small flux, intermittency and the presence of non-turbulent physics (e.g. gravity waves and radiative flux divergence). Therefore, it is difficult to determine boundary layer height experimentally or numerically (Stoll and Porte-Agel, 2009). In this study, the initial boundary layer height as the surface layer transitions from stable to unstable is necessary to define the starting value of h for the following calculations. The calculation of atmospheric boundary layer height at night was not included in these attempts to improve the model. The atmospheric boundary layer height for night time was measured by lidar. The lidar detected that the height of the atmospheric boundary layer at the area of study was around 400 m. This was due to urban activities at night that cause an increase in heat capacity and an increase of the atmospheric boundary layer height. In this case, the atmospheric boundary layer height at night was determined using vertical velocity variance. Atmospheric boundary layer height from lidar vertical velocity variance was achieved by plotting the vertical velocity time series and calculating the vertical velocity variance. The variance can be used to detect the turbulence in the boundary layer. Turbulence in the vertical velocity variance is shown by the value of the variance above a threshold value. In this study, the value 0.2 m^2/s^2 times by the variance maximum was used as the threshold to indicate the atmospheric boundary layer height. The boundary layer height calculation is not very sensitive to the value chosen.

Although the transition time from night time to day time, where sensible heat flux changes from negative to positive (Lapworth, 2006), were different for each of six days in this study, 08:00 was chosen as the boundary layer did not begin to grow before this time in any cases. The boundary layer height from this time was used as the initial value of h in the model runs. These initial values of h can be seen in Table 2.

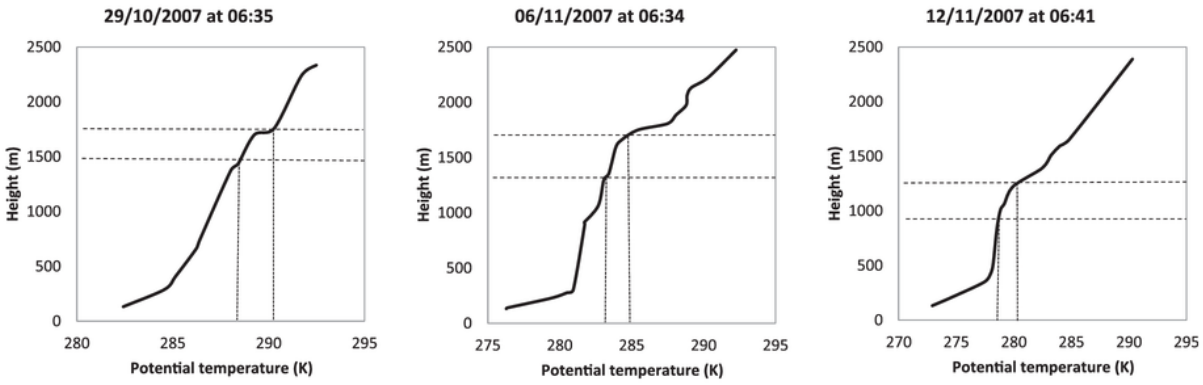

Fig. 9. Potential temperature in Larkhill for three days. Note: The dashed lines are the range for calculating gamma, the lower threshold is the maximum height of h lidar measurement on that day and the upper threshold is height below 2000 m of radiosonde data. Temperature profile data was not available for 04/11/2007.

Table 1
Gamma used for calculation of atmospheric boundary layer height.

Date	Gamma (km^{-1})
29/10/2007	0.0038
04/11/2007	0.0030[a]
06/11/2007	0.0028
12/11/2007	0.0037

[a] There was no data for this date, so gamma was assumed and chosen from one of gamma used in this study to give the best result for the combined model.

Table 2
The initial *h* used for calculation of atmospheric boundary layer height.

Date	The initial *h* (meter)
29/10/2007	210
04/11/2007	295
06/11/2007	575
12/11/2007	420

Note: the initial *h* were measured by lidar (were obtained from lidar vertical velocity variance at 08:00).

2.8. Calculation of atmospheric boundary layer height

Many models can be used to calculate of the atmospheric boundary layer height, such as Stull (1976), Troen and Mahrt (1986), and Batchvarova and Gryning (1991). In Stull (1976) predicted the atmospheric boundary layer height using an entrainment equation which was based on the turbulent kinetic energy equation for mixed layer. The model was in a good agreement with the observations for the Great 1953 Plains experiment, the 1967 Australian Wangara experiment, and the 1972 Puerto Rican tropical experiment (Stull, 1976). Troen and Mahrt (1986) developed a simple model to predict the growth of the atmospheric boundary layer height. The model used a bulk Richardson number which was modified by including the influence of thermals. The model performed reasonably well in the cases of weak surface heat flux and the transition between stable and unstable condition. Batchvarova and Gryning (1991) presented a simplified model for the atmospheric boundary layer height. In the model, the potential temperature was assumed to be uniform with height in the atmospheric boundary layer with a thin inversion in the entrainment zone. The model can be used if the time variation of sensible heat flux, friction velocity and the height variation of the temperature gradient are available. The model gave good results for the

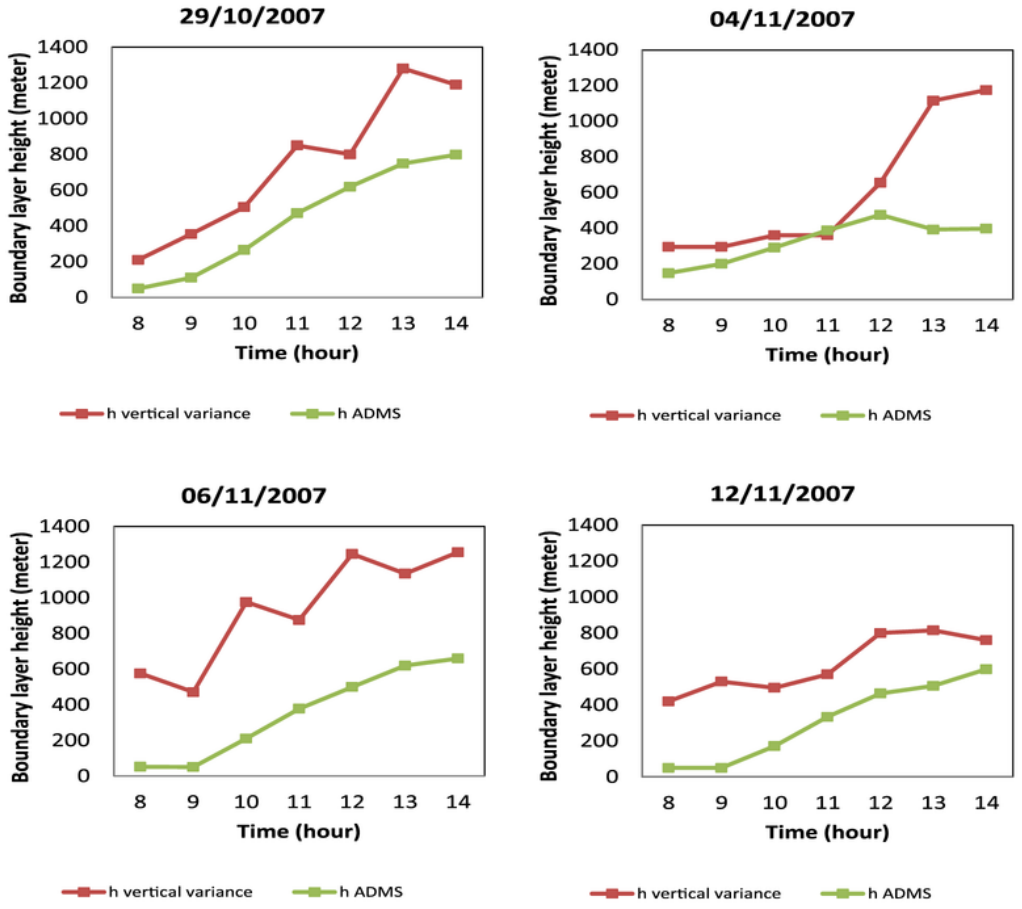

Fig. 10. Comparison of the atmospheric boundary layer height between ADMS and lidar vertical velocity variance (the green line is *h* determined by ADMS 4 and the dark brown line is *h* determined by lidar vertical velocity variance). (For interpretation of the references to colour in this figure legend, the reader is referred to the web version of this article.)

growth of the atmospheric boundary layer height, during unstable conditions.

The model from Batchvarova and Gryning (1991) was chosen for this study for several reasons. Firstly, the model was appropriate to this study, to predict the growth of atmospheric boundary layer height in unstable conditions. The model is simple and all input parameters can be obtained either from measurements or calculations. This model was also used in previous studies by Nardino et al. (2001) and Argentini et al. (2005). Nardino et al. (2001) used this model to calculate atmospheric boundary layer height in a campaign in the Po Valley, Italy, and compared with the data measurements from radio sounding and sodar. They found a good agreement between the model and the measurements. Meanwhile, Argentini et al. (2005) used this model to predict atmospheric boundary layer height at the Plateau site of Dome C, Antarctica and compared with sodar measurements. They argued that the model was satisfactory and agreed with the data from sodar measurement in predicting the atmospheric boundary layer height.

The equation from Batchvarova and Gryning (1991) used in this study is as follow:

$$\left\{\frac{h^2}{(1+2A)h-2B\kappa L}+\frac{Cu_*^2T}{\gamma g[(1+A)h-B\kappa L]}\right\}\frac{dh}{dt}=\frac{\left(\overline{w'\theta'}\right)_s}{\gamma} \quad (11)$$

$$w'\theta'_s = QM/(\rho\ c_p) \quad (12)$$

where h is the atmospheric boundary layer, u_* is the friction velocity, g/T is the buoyancy parameter, κ is the von Karman constant, L is the Monin-Obukhov length, γ is the potential temperature gradient above h, w_s = - div h (div is the horizontal divergence), $(\overline{w'\theta'})_s$ is the vertical kinematic heat flux at the surface, A, is parameterization constant ($A = 0.2$)

B is parameterization constant ($B = 2.5$, $B = 5$), and C is parameterization constant ($C = 8$).

The Batchvarova and Gryning (1991) model is derived from two terms. The first term on the left is calculated from the combined effect of mechanical and convective turbulence, and the second term is calculated due to the spin-up effect (the local change of turbulence kinetic energy (TKE) due to entrainment of air with little TKE from the air above the atmospheric boundary layer (Gryning, 2005)). Calculation of h using the Batchvarova and Gryning (1991) model was achieved using numerical integration. In this study, Simpson's rule was used to calculate h using numerical integration (Griffiths and Smith, 1991). The input data required for this calculation were surface roughness length, friction velocity, Monin-Obukhov length, sensible heat flux, the potential temperature above the atmospheric boundary layer, and the night time boundary layer height.

3. Results and discussion

3.1. Comparison atmospheric boundary layer height from dispersion model and lidar

Comparison of atmospheric boundary layer height from the atmospheric dispersion model and lidar vertical velocity variance was undertaken. The variance can be used to detect the turbulence in the boundary layer. Turbulence in the vertical velocity variance is shown by the value of the variance above a threshold value. In this study, the value 0.2 m^2/s^2 × the variance maximum was used as the threshold to indicate the atmospheric boundary layer height. This method was used because some of the variance maximum values were very high and some of them were very low, and this threshold produced the best prediction of the atmospheric boundary layer height.

Comparison between atmospheric dispersion model and lidar vertical velocity variance were conducted for four clear days: 29th, 4th, 6th, and 12th November 2007 in the day time from 08:00 to 14:00 local time. The ADMS 4 output compared here is for Northolt Meteorological data. Each hour data of lidar vertical velocity variance constitutes the average of both five minutes data before the hour and five minutes data after the hour. The averaging of this ten minutes data is aimed to decrease the noise detected from lidar measurements.

It can be seen in Fig. 10 that the atmospheric boundary layer heights (h) predicted by ADMS 4 are under predicted compared with lidar measurements. In the early morning (08:00), ADMS 4 predicts an atmospheric boundary layer height of less than 200 m. This is not appropriate with h in urban areas where h is very seldom less than 200 m at the morning transition time (Fisher et al., 2005; Lu and Arya, 1997). Meanwhile, lidar vertical velocity variance detects the atmospheric boundary layer height to be 200 m or higher at this time. In the afternoon (between 12:00 and 14:00), h predicted by ADMS 4 is around 800 m. Meanwhile, h predicted by lidar vertical velocity variance varies between 800 m and 1200 m. So the conclusion is that h prediction by ADMS 4 is too low in urban areas where h can reach more than 1000 m (Dupont et al., 1999), depending upon the meteorological conditions at that time.

From comparison of ADMS 4 and lidar data in Fig. 10, it can be seen that ADMS 4 has limitations. This might be due to the fact that the parameters used in ADMS 4 are not suitable for urban areas (in this case central London). The friction velocity formulation in ADMS 4 is based on surface wind velocity components, stability and surface roughness. In urban areas, the surface roughness elements are non-uniform. However, ADMS 4 does not consider the effect of non-uniformities in the surface properties (Thomson, 2009).

In stable conditions (before 08:00 in the morning), ADMS predicts h to be lower than 200 m, meanwhile lidar backscatter (not shown) and lidar vertical velocity variance determine h to be higher than 200 m. This is caused by ADMS setting h value to the minimum value (50 m) under what it determines to be stable conditions This then influences the value of h at the time of the morning transition, whereas urban surfaces stay warm in the night caused by urban activities. Urban activities cause sensible heat flux in urban areas to be higher than in rural areas (Fisher et al., 2005), and this will lead to a value of h higher than the minimum value of ADMS prediction (50 m). Table 3 shows difference between ADMS 4 and lidar boundary layer height calculations. It can be seen correlations between ADMS 4 and lidar were higher than the critical value, 0.754 for a confidence level at 95%. except on 04/11/2007. This means correlation between ADMS 4 and lidar was significant, except for 04/11/2007. In general, it can be concluded that the overall pattern of h predicted by ADMS 4 was similar to lidar. Likewise, these data show that the difference is variable, between 288 m and 581 m. The largest difference was on 6th November 2007. The size of this difference is such that it is similar in scale to the actual ADMS 4 h values. This means, although there was a statistically significant different between ADMS 4 and lidar, there was an height gap

Table 3
Statistical analysis (Pearson correlation and mean absolute difference) between ADMS and lidar.

Date	Pearson correlation	Mean absolute difference (meter)
29/10/2007	0.971	304
04/11/2007	0.617	288
06/11/2007	0.915	581
12/11/2007	0.914	317

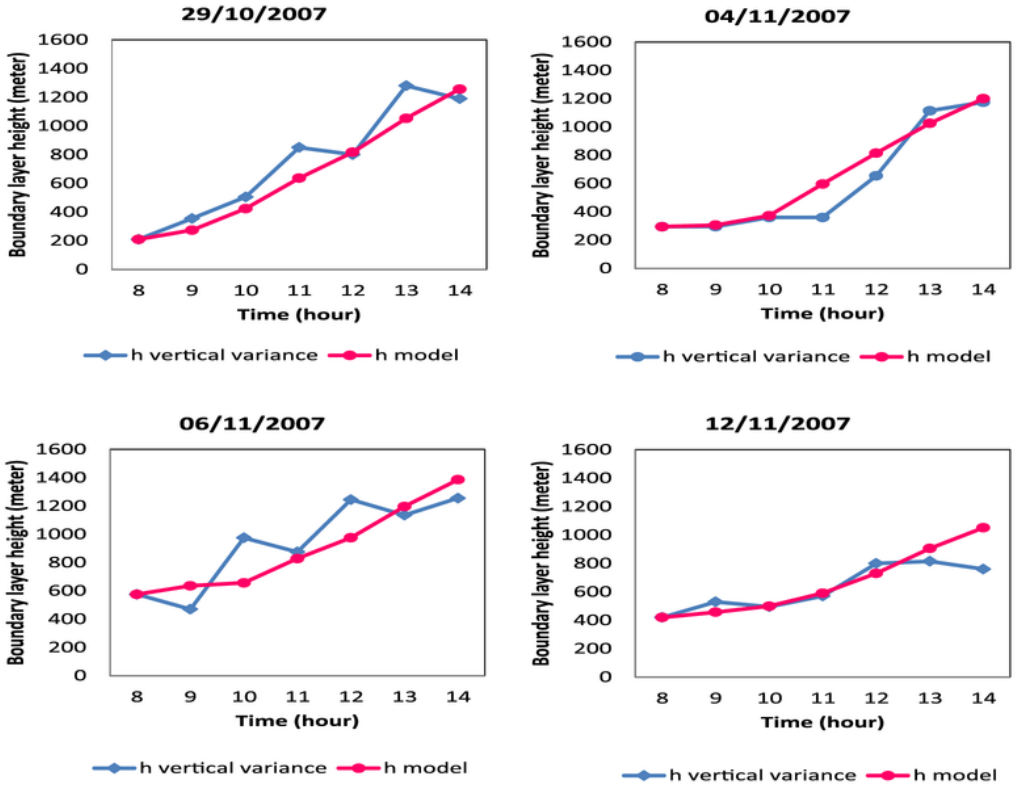

Fig. 11. Comparison *h* model against *h* lidar vertical velocity variance.

between them (ADMS 4 predicted the atmospheric boundary layer height was just a half of the measurements of lidar).

3.2. Comparison atmospheric boundary layer height from combined model and lidar

Using the combined model developed in section 2 of this paper a comparison is made for the days discussed previously between *h* from the combined model calculation and *h* from lidar vertical velocity variance as derived previously (Fig. 11). The figure shows *h* values from the model and lidar vertical velocity variance from 08:00 to 14:00. It can be seen that *h* model is close to *h* lidar, although the values of *h* model in the morning are slightly lower and after midday are slightly higher. The difference between *h* lidar and *h* model is caused by *h* lidar having different patterns each day (sometimes *h* lidar increases after midday and sometimes it decreases). Meanwhile *h* model tends to have similar pattern, namely monotonic increase with time. It should be noted that the Batchvarova and Gryning (1991) model was developed and validated for morning growth of the boundary layer. As the day progresses competing factors start to affect the boundary layer growth and it is more common for the boundary layer growth to slow down as it approaches its maximum value. These competing factors are not incorporated into this combined model.

Statistical analysis of the combined *h* model was assessed using correlation (using Pearson correlation) and by calculation of the difference (Table 4). All correlation coefficients were significant ($P < 0.05$). For the four days predictions, mean absolute difference varied between 76 m and 142 m. These values are less than difference between ADMS 4 and the lidar.

4. Conclusions

An improvement of atmospheric boundary layer height estimation was achieved using a surface model from Grimmond and Oke (1999) combined with the atmospheric boundary layer height model from Batchvarova and Gryning (1991). Parameters for calculating the atmospheric boundary layer height were surface roughness, friction velocity, sensible heat flux and potential temperature gradient above the atmospheric boundary layer. The surface model was employed to calculate the surface roughness of the area study (central London). In this case, the area of study was characterized by dense tall building. This model was chosen because the calculation can be determined without a need of tall instrumented tower. The database of roughness elements was derived from airborne lidar and the surface roughness from this was used as an input in the atmospheric boundary layer height model.

Some parameters (friction velocity, sensible heat flux, and potential temperature gradient above the atmospheric boundary layer) were employed to calculate the atmospheric boundary layer

Table 4
Statistical analysis (significance correlation and mean absolute difference) between model and lidar.

Date	Pearson correlation	Mean absolute difference (meter)
29/10/07	0.961	98
04/11/07	0.959	76
06/11/07	0.816	142
12/11/07	0.880	78

height from the Batchvarova and Gryning (1991) model. Friction velocity was calculated as a function of wind speed, surface roughness and height. Wind speeds were measured using lidar and from Northolt Meteorological Station. Sensible heat flux was calculated as a modified sensible heat flux using data from Northolt Meteorological Station. Radiosonde data from Larkhill were used for calculation of gamma.

The estimation of atmospheric boundary layer height from the combined models was carried out using specific parameters (surface roughness length, friction velocity, Monin-Obukhov length, sensible heat flux and potential temperature gradient above the atmospheric boundary layer). Surface roughness length was calculated using morphometric methods. The surface roughness length from this calculation was higher than surface roughness length from ADMS 4 for urban areas setting. Friction velocity was estimated using two methods; the mean wind speed and iteration. The comparison of both methods concluded that friction velocities of the mean wind speed were higher than the iteration method, but gave similar results for the atmospheric boundary layer height (h). This is because values of Monin–Obukhov used for h prediction were similar, whereas friction velocity influences Monin–Obukhov length and *vice versa*. Monin–Obukhov length was calculated using iteration. For sensible heat flux, modification was made to Northolt sensible heat flux data, which had characteristics of open grass, so as to be more suitable for urban areas. Then, potential temperature gradient above the atmospheric boundary layer was calculated from temperature vertical data from Larkhill.

The atmospheric boundary layer height predicted using combined model was compared with the atmospheric boundary layer height measurements obtained by lidar vertical velocity variance showing good agreement. The implications of these findings for air pollution modelling are that the combined model applied here can improve the prediction of the atmospheric boundary layer height (h) in the ADMS Met pre-processor providing more accurate outputs in model applications.

Acknowledgements

This study was funded by Indonesian Government (Indonesian Directorate General of Higher Education). We also acknowledge to UK Met Office for providing the meteorological data for running ADMS 4. Thanks to Dr. Sven-Erik Gryning from Wind Energy Department, Riso National Laboratory for Sustainable Energy Technical, University of Denmark, for his help through personal discussions, and Dr. Sabine von Hunerbein, Salford University, for providing the surface meteorological data and for support with the research.

References

American Meteorology Society (AMS), 2009. Glossary of Meteorology. http://amsglossary.allenpress.com/glossary.

Argentini, S., Viola, A., Sempreviva, A.M., Petenko, I., 2005. Summer boundary-layer height at the plateau site of dome C, Antarctica. Boundary Layer Meteorol. 115, 409–422.

Arya, S.P., 2005. Micrometeorology and atmospheric boundary layer. Pure Appl. Geophys. 162, 1721–1745.

Batchvarova, E., Gryning, S.E., 1991. Applied model for the growth of the daytime mixed layer. Boundary Layer Meteorol. 56, 261–274.

Barlow, J., Dunbar, T., Nemitz, E.G., Wood, C.R., Gallagher, M.W., Davies, F., O'Connor, E., Harrison, R.M., 2011. Boundary layer dynamics over London, UK, as observed using doppler lidar during REPARTEE-II. Atmos. Chem. Phys. Discuss. 11, 2111–2125.

Bozier, K., Davies, F., Collier, C.G., 2006. Autonomous doppler lidar system for atmospheric boundary layer monitoring. In: Proceedings of Photon 06, Manchester, UK, 4–7 September 2006.

Bozier, K.E., Pearson, G.N., Collier, C.G., 2007. Evaluation of A New autonomous doppler lidar system during the Helsinki International Testbed field campaign. In: Third Symposium on Lidar Atmospheric Applications, American Meteorology Society Annual Meeting, San Antonio, Texas, 15–18 January 2007.

British Atmospheric Data Centre (BADC), 2010. Larkhill Radiosonde Data. http://badc.nerc.ac.uk/ (accessed 02.01.10.).

Carruthers, D.J., Holroyd, R.J., Hunt, J.C.R., Weng, W.S., Robins, A.G., Apsley, D.D., Thompson, D.J., Smith, F.B., 1994. UK-ADMS: a new approach to modelling dispersion in the Earth's atmospheric boundary layer. J. Wind Eng. Ind. Aerodyn. 52, 139–153.

Dandao, A., Tombrou, M., Schafer, K., Emeis, S., Protonotariou, A.P., Bossioli, E., Soulakellis, N., Suppan, P., 2009. A comparison between modelled and measured mixing-layer height over Munich. Boundary Layer Meteorol. 131, 425–440.

Davies, F., Middleton, D.R., Bozier, K.E., 2007. Urban air pollution modelling and measurements of boundary layer height. Atmos. Environ. 41, 4040–4049.

Department for Environment Food and Rural Affairs (DEFRA), 2007. The Air Quality Strategy for England, Scotland, Wales and Northern Ireland, vol. 2. Crown Copyright, Norwich, pp. 1–275. www.defra.gov.uk.

Dupont, E., Menut, L., carissimo, B., Pelon, J., Flammant, P., 1999. Comparison between the atmospheric boundary layer in Paris and its rural suburbs during the ECLAP experiment. Atmos. Environ. 33, 979–994.

Dupont, S., Otte, T.L., Ching, J.K.S., 2004. Simulation of meteorological Fields within and above urban and rural Canopies with A Mesoscale model (MM5)*. Boundary Layer Meteorol. 113, 111–158.

Fatogoma, O., Jacko, R.B., 2002. A model to estimate mixing height and its effects on ozone modeling. Atmos. Environ. 36, 3699–3708.

Fisher, B., Joffre, S., Kukkonen, J., Piringer, M., Rotach, M., Schatmann, M., 2005. Meteorology Applied to Urban Air Pollution Problems. Final Report of COST Action 715. Demetra Ltd Publishers, Bulgaria, pp. 1–24.

Griffiths, D.V., Smith, I.M., 1991. Numerical Methods for Engineers. Blackwell Scientic Publications, London, UK, pp. 171–173.

Grimmond, C.S.B., Oke, T.R., 1999. Aerodynamic properties of urban areas derived from analysis of surface form. J. Appl. Meteorol. 38, 1262–1292.

Gryning, S.E., 2005. The Height of the Atmospheric Boundary Layer during Unstable Conditions. Riso-R Report, ISBN 87-550-3479-9 (Internet).

He, Q.S., Mao, J.T., Chen, J.Y., Hu, Y.Y., 2006. Observational and modeling studies of urban atmospheric boundary layer height and its evolution mechanisms. Atmos. Environ. 40, 1064–1077.

Kato, S., Yamaguchi, Y., 2005. Analysis of urban heat-island effect using ASTER and ETM+ data: separation of anthropogenic heat discharge and natural heat radiation from sensible heat flux. Remote Sens. Environ. 99 (2005), 44–54.

Lapworth, A., 2006. The morning transition of the nocturnal boundary layer. Boundary Layer Meteorol. 119, 501–526.

Lu, J., Arya, S.P., 1997. A laboratory study of the urban heat island in a calm and stably stratified environment. Part I: temperature field. J. Appl. Meteorol. 36, 1377–1391.

MIMAS, 2010. Building Height Data for Central London. http://landmap.mimas.ac.uk/ (accessed 15.01.10.).

Nardino, M., Calzolari, F., Geordiadis, T., Levizzani, V., Sozzi, R., 2001. Computing of the mixed layer height through the Gryning–Batchvarova model and comparison with experimental data during MAP-SOP. MAP Newsl. 15, 156–159. MeteoSwiss, CH-8044 Zurich.

Pearson, G., Davies, F., Collier, C.G., 2009. An analysis of the performance of the UFAM pulsed doppler lidar for observing the boundary layer. J. Atmos. Ocean. Technol. 26, 240–250.

Raupach, M.R., 1991. Vegetation atmosphere interaction in homogeneous and heterogeneous terrain: some implications of mixed layer dynamics. Vegetation 91, 105–120.

Raupach, M.R., 1992. Drag and drag partition on rough surfaces. Boundary Layer Meteorol. 60, 375–395.

Sidle, C., Kidd, J., Ng, B., McVay, M., Heptinstall, N., Shi, J.P., 2004. A comparison of boundary layer heights in atmospheric dispersion models and possible consequences for modelling emissions from tall stacks. In: 9th Int. Conf on Harmonisation within Atmospheric Dispersion Modelling for Regulatory Purposes, Garmisch-Partenkirchen, Germany, 1–4 June, 2004.

Stoll, R., Porte-Agel, F., 2009. Surface heterogeneity effects on regional-scale fluxes in stable boundary layers: surface temperature transitions. J. Atmos. Sci. 66, 412–431.

Stull, R.B., 1976. Mixed layer depth model based on turbulent energetics. J. Atmos. Sci. 33, 1268–1278.

Stull, R.B., 1988. An Introduction to Boundary Layer. Kluwer Academic Publishers, Netherlands, pp. 2–25.

Thomson, D.J., 2009. The Met Input Module ADMS 4 Technical Specification, P05/01P/09. Cambridge Environmental Research Consultant, Maret. http://www.cerc.co.uk/software/pubs/ADMS4TechSpec/P05_01.pdf.

Troen, I.B., Mahrt, L., 1986. A simple model of the atmospheric boundary layer; sensitivity to surface evaporation. Boundary Layer Meteorol. 37, 129–148.

U.S. Environmental Protection Agency (U.S. EPA), 2008. Air Quality Planning and Standards, Air Quality Modelling. http://www.epa.gov/oar/oaqps/modeling.html (accessed 11.06.09.).

World Health Organisation (WHO), 2008. Air Quality and Health. http://www.who.int/mediacentre/factsheets/313/en/index.html (accessed 07.06.09.).

Wieringa, J., 1993. Representative roughness parameters for homogeneous terrain. Boundary Layer Meteorol. 63, 323–363.

Wulfmeyer, V., Behrendt, A., Bauer, H.-S., Kottmeier, C., Corsmeier, U., Blyth, A., Craig, G., Schumann, U., Hagen, M., Crewell, S., Girolamo, P.D., Flamant, C.,

Miller, M., Montani, A., Mobbs, S., Richard, E., Rotach, M.W., Arpagaus, M., Russchenberg, H., Schlussel, P., Konig, M., Gartner, V., Steinacker, R., Dorninger, M., Turner, D.D., Weckwerth, T., Hense, A., Simmer, C., 2008. The convective and orographically induced precipitation study (COPS): a research and development project of the world weather research program for improving quantitative precipitation forecasting in low-mountain regions. Bull. Am. Meteorol. Soc. 89, 1477–1486.

A combined model for improving estimation of atmospheric boundary layer height

ORIGINALITY REPORT

5%	0%	5%	0%
SIMILARITY INDEX	INTERNET SOURCES	PUBLICATIONS	STUDENT PAPERS

PRIMARY SOURCES

1	Grimmond, C. S. B., and T. R. Oke. "Aerodynamic Properties of Urban Areas Derived from Analysis of Surface Form", Journal of Applied Meteorology, 1999. Publication	5%

Exclude quotes	On	Exclude matches	< 3%
Exclude bibliography	On		